HHS Public Access

Author manuscript

Comput Chem Eng. Author manuscript; available in PMC 2022 March 04.

Published in final edited form as:

Comput Chem Eng. 2022 February ; 158: . doi:10.1016/j.compchemeng.2021.107617.

*Corresponding author at: Chemical & Biomolecular Engineering Department, University of Houston, 4226 MLK Blvd, Houston TX 77004, United States. nikolaou@uh.edu (M. Nikolaou).

Author contributions

In absence of specific instructions and in research fields where it is possible to describe discrete efforts, the Publisher recommends authors to include contribution statements in the work that specifies the contribution of every author in order to promote transparency. These contributions should be listed at the separate title page.

Conceptualization – Ideas; formulation or evolution of overarching research goals and aims.
Iordanis Kesisoglou
Vincent H Tam
Michael Nikolaou

Data curation – Management activities to annotate (produce metadata), scrub data and maintain research data (including software code, where it is necessary for interpreting the data itself) for initial use and later re-use.
Iordanis Kesisoglou
Vincent H Tam
Michael Nikolaou

Formal analysis – Application of statistical, mathematical, computational, or other formal techniques to analyze or synthesize study data.
Iordanis Kesisoglou
Michael Nikolaou

Funding acquisition – Acquisition of the financial support for the project leading to this publication.
Vincent H Tam
Michael Nikolaou

Investigation – Conducting a research and investigation process, specifically performing the experiments, or data/evidence collection.
Iordanis Kesisoglou

Methodology – Development or design of methodology; creation of models.
Iordanis Kesisoglou
Michael Nikolaou

Project administration – Management and coordination responsibility for the research activity planning and execution.
Vincent H Tam
Michael Nikolaou

Resources – Provision of study materials, reagents, materials, patients, laboratory samples, animals, instrumentation, computing resources, or other analysis tools.
Vincent H Tam
Michael Nikolaou
Andrew P. Tomaras

Software – Programming, software development; designing computer programs; implementation of the computer code and supporting algorithms; testing of existing code components.
Matlab
Mathematica

Supervision – Oversight and leadership responsibility for the research activity planning and execution, including mentorship external to the core team.
Vincent H Tam
Michael Nikolaou

Validation – Verification, whether as a part of the activity or separate, of the overall replication/reproducibility of results/experiments and other research outputs.
Iordanis Kesisoglou

Visualization – Preparation, creation and/or presentation of the published work, specifically visualization/data presentation.
Iordanis Kesisoglou

Writing – original draft – Preparation, creation and/or presentation of the published work, specifically writing the initial draft (including substantive translation).
Iordanis Kesisoglou
Michael Nikolaou

Writing – review & editing – Preparation, creation and/or presentation of the published work by those from the original research group, specifically critical review, commentary or revision – including pre- or post-publication stages.
Iordanis Kesisoglou
Vincent H Tam
Michael Nikolaou

Declaration of Competing Interest

All contributing authors have no conflict of interest.

Discerning in vitro pharmacodynamics from OD measurements: A model-based approach

Iordanis Kesisoglou[a], **Vincent H Tam**[b,a], **Andrew P. Tomaras**[c], **Michael Nikolaou**[a,*]

[a]Chemical & Biomolecular Engineering Department, University of Houston, 4226 MLK Blvd, Houston TX 77004, United States

[b]Department of Pharmacy Practice and Translational Research, University of Houston, 4349 MLK Blvd, Houston TX 77204, United States

[c]BacterioScan Inc. 2210 Welsch Industrial Ct, St. Louis, MO 63146 United States

Abstract

Time-kill experiments can discern the pharmacodynamics of infectious bacteria exposed to antibiotics in vitro, and thus help guide the design of effective therapies for challenging clinical infections. This task is resource-limited, therefore typically bypassed in favor of empirical shortcuts. The resource limitation could be addressed by continuously assessing the size of a bacterial population under antibiotic exposure using optical density measurements. However, such measurements count both live and dead cells and are therefore unsuitable for declining populations of live cells. To fill this void, we develop here a model-based method that infers the count of live cells in a bacterial population exposed to antibiotics from continuous optical-density measurements of both live and dead cells combined. The method makes no assumptions about the underlying mechanisms that confer resistance and is widely applicable. Use of the method is demonstrated by an experimental study on *Acinetobacter baumannii* exposed to levofloxacin.

Keywords

Mathematical modeling; Pharmacodynamics; Multi-drug resistant bacteria; Combination therapy

1. Introduction

Bacterial resistance to antibiotics has grown to pose a serious threat to human health (Neu 1992, Davies 1994, Levy and Marshall 2004, Morens, Folkers et al. 2004, Fischbach and Walsh 2009, Blair, Webber et al. 2015, Blaser 2016), Development of new antibiotics or other antimicrobials and effective use of existing ones are essential for combating antibiotic resistance (Wang and Lipsitch 2006, Fischbach and Walsh 2009, Huh and Kwon 2011, Lewis 2013, O'Connell, Hodgkinson et al. 2013, Czaplewski, Bax et al. 2016, Crofts, Gasparrini et al. 2017, Blanquart, Lehtinen et al. 2018). For both development and clinical use of antibiotics, aids in guiding the selection of effective antibiotics and corresponding dosing regimens are essential both for direct therapeutic purposes and for mitigating the emergence of resistant bacterial strains (Tam and Nikolaou, 2011a). A standard such aid is experiments in which a bacterial population is exposed to an antibiotic at different time-invariant concentrations, over a period of time. In the simplest case of such an experiment,

an observation is made at the end of the experiment and the minimal concentration of an antibiotic capable of inhibiting growth of the studied bacterial population (minimum inhibitory concentration, MIC) at that point is assessed. While simple and universally used, MIC captures only a small fraction of the information that could be gleaned from such an experiment (see Tam and Nikolaou (2011) and references therein). For example, as such an experiment progresses over time, the size of the bacterial population can be assessed at distinct points in time, typically by quantitative culture (plating) methods (Sanders 2012). Processing of the (time-kill) experimental data thus collected can better help guide the design of effective antibiotic dosing regimens. Such data processing can be heuristic, e.g. through estimation of MIC and/or other pharmacodynamic indicators (Andrews 2001, Mouton, Dudley et al. 2005, Wiegand, Hilpert et al. 2008), or by building more detailed mathematical models, particularly when a bacterial population comprises subpopulations of varying degrees of resistance (Lipsitch and Levin 1997, Giraldo, Vivas et al. 2002, Nikolaou and Tam, 2006; Tam and Nikolaou, 2011b, Bhagunde, Nikolaou et al. 2015).

While plating used with time-kill experiments to assess the size of a surviving bacterial population exposed to antibiotics is a standard tool, it is time-consuming, labor-intensive, and produces a limited number of data points, needed for reliable predictions. These shortcomings make plating difficult to use in situations where time or resources are limited yet reliable results are needed for quick decision making, e.g. in a clinical setting.

Alternatives to traditional plating can be considered for measurement of a bacterial population size, each with its distinct advantages but also limitations for the intended use: Quantitative polymerase chain reaction (PCR) (Kralik and Ricchi 2017, Ricchi, Bertasio et al. 2017), fluorescence microscopy (Wang, Hammes et al. 2010, Hasan, Alam et al. 2016), and enzyme-linked immunosorbent assay (ELISA) (Gracias and McKillip 2004) have bearable set up cost but can take prohibitively long (from hours to days); fluorescence-based microplate reader (Alakomi, Mättö et al. 2005, Pascaud, Amellal et al. 2009, Feng, Wang et al. 2014) and flow cytometry (FCM) (Imade, Badung et al. 2005, Wang, Hammes et al. 2010, Ou, McGoverin et al. 2017) take minutes for bacteria detection and have low cost per test but they have again high set up costs: and fiber-based fluorescence spectroscopy (Guo, McGoverin et al. 2017) allows detection in minutes with a relatively low error, low setup cost, and cost per test, but a sample taken must be first taken and stained for each measurement.

Finally, yet another alternative to plating for essentially continuous assessment of the size of a bacterial population relies on optical density (OD) measurements of a bacterial population in suspension (spectrophotometry) (McMeekin, Olley et al. 1993, López, Prieto et al. 2004, (Mytilinaios et al., 2012)). OD measurements rely on well known principles and can easily and inexpensively provide a continuous stream of data in real time. While these features are appealing, OD measurements also have an important limitation: They count both live and dead cells in a bacterial population, as both kinds of cells produce an optical signal by blocking/absorbing light. Therefore, OD measurements are typically suitable for monitoring a *growing* bacterial population, but cannot keep track of a *declining* population that exhibits patterns such as those shown in Fig. 1. Indeed, when a bacterial population is in decline (in response to antibiotic exposure) OD measurements produce a continuous *non-*

decreasing signal, because the sum of live and dead cells is non-decreasing. In particular, OD measurements are of little value in the important case of time-kill experiments with bacterial populations comprising subpopulations of varying degrees of antibiotic resistance. This is because, at certain concentrations of the antibiotic, regrowth of the population could occur, due to early decline of susceptible subpopulations and simultaneous growth of subpopulations resistant to the antibiotic, as shown in Fig. 1. In that figure, the thick curves corresponding to both live and dead cell counts of a *growing* bacterial population (at low antibiotic concentrations) provide enough qualitative information on live cell counts (thin dashed lines) by inspection. However, for populations in regrowth, in retarded regrowth, or in decline (Fig. 1), mere inspection of the thick lines offers no indication about the trend of live cell counts (thin dashed lines) and offers hardly any clues towards the design of an effective therapeutic treatment. It is for these situations, which are essential from a therapeutic view-point, that we propose here a mathematical model-based method to circumvent the serious limitations of OD methods while retaining their advantages.

The approach taken to build the proposed mathematical model structure starts with equations that capture the effect of an antibiotic on a heterogeneous bacterial population comprising subpopulations of varying degrees of resistance, as shown qualitatively in Fig. 1 (Nikolaou and Tam 2006, Bhagunde, Nikolaou et al. 2015). That model structure makes minimal assumptions about the underlying mechanisms that confer resistance, and can be used with one or more antibiotics in combination. The model structure is extended here to describe the antibiotic effect on the entire cell count in a bacterial population, namely on both live and dead cells, as illustrated in Fig. 1. As detailed below, the proposed general model structure relies on minimal assumptions and includes a small number of parameters that can be easily estimated based on experimental data.

In the rest of the paper, we first provide the basic equations that constitute the starting point for the Results. These results are developed in the Mathematical modeling section and illustrated through an experimental study presented in the Experimental section. Finally, conclusions and recommendations for further study are presented.

2. Materials and methods

2.1. Background on mathematical modeling

When a bacterial population is exposed to an antibiotic, the population experiences kill rates $r \geq 0$ (Wagner 1968, Jusko 1971, Giraldo, Vivas et al. 2002) which vary over subpopulations of the overall population, as these subpopulations have different susceptibilities to the antibiotic at a given concentration (Lipsitch and Levin 1997, Giraldo, Vivas et al. 2002). If such a heterogeneous bacterial population is exposed to an antibiotic at a time-invariant concentration, the distribution of kill rates changes over time, as susceptible bacteria are killed faster than less susceptible (more resistant) bacteria, thus changing the pharmacodynamics of the antibiotic/bacteria interaction. The least susceptible (most resistant) subpopulation eventually becomes dominant and experiences either eradication or regrowth, depending on whether the natural growth rate of that most resistant subpopulation is lower or higher, respectively, than the kill rate induced on that subpopulation by the antibiotic at that concentration (Hill 1910, Wagner 1968, Jusko 1971, Giraldo, Vivas et al.

2002). Under non-demanding assumptions, the related dynamics is captured well by general equations developed by Nikolaou and Tam (2006) and Bhagunde, Nikolaou et al. (2015), according to which the size of a heterogeneous bacterial population exposed to one or more antibiotics at constant concentration over time is well approximated by the equation

$$\ln\left[\frac{N_{\text{live}}(t)}{N_0}\right] = (K_g - r_{\min})t + \lambda\left(e^{-at} - 1\right) - \ln \left[1 + K_g \frac{N_{\text{live}}(0)}{N_{\max}} \int_0^t \exp\left[(K_g - r_{\min})\tau + \lambda(e^{-a\tau} - 1)\right] d\tau\right] \quad (1)$$

and the kill rate average and variance over time are well approximated by the equations

$$\mu(t) = r_{\min} + (\mu(0) - r_{\min})\exp\left[-\frac{\mu(0) - r_{\min}}{\lambda}t\right] = r_{\min} + \lambda a e^{-at} \quad (2)$$

$$\sigma(t)^2 = \frac{(\mu(0) - r_{\min})^2}{\lambda}\exp\left[-\frac{\mu(0) - r_{\min}}{\lambda}t\right] = \lambda a^2 e^{-at} \quad (3)$$

where

$N_{\text{live}}(t)$ is the live bacterial population size with initial value N_0

K_g is the physiological net growth rate of the entire bacterial population, common for all subpopulations

$r_{\min}$ is the kill rate induced by the antibiotic on the most resistant (least susceptible) subpopulation

$N_{\max}$ is the maximum size of a bacterial population reaching saturation under growth conditions

$\mu(t)$ is the kill rate average over the bacterial population at time t

$\sigma(t)^2$ is the kill rate variance over the bacterial population at time t

$\lambda > 0,\ a > 0$ are constants associated with the initial decline of the average kill rate of the population, and correspond to the Poisson distributed variable $\frac{r - r_{\min}}{a}$ with average and variance equal to λ.

Note that the above two equations for $N_{\text{live}}(t)$ and $\mu(t)$ have been derived with essentially no assumptions about the mechanisms that may confer bacterial resistance. The parameters K_g, $r_{\min}$, λ, a, $N_{\max}$ that appear in the above expressions for $N_{\text{live}}(t)$ and $\mu(t)$ can be estimated from time-kill experiments that produce measurements of $N_{\text{live}}(t)$ over time at various set concentrations of the antibiotic.

Estimates of parameters such as K_g and $r_{\min}$ are essential for guiding the design of effective dosing regimens. For example, it has been shown (Nikolaou, Schilling et al. 2007) that an antibiotic injected periodically and following pharmacokinetics of exponential decay during each period, T, will eradicate a heterogeneous bacterial population when $\frac{1}{T}\int_0^T r_{\min}(C(t))dt > K_g$ where $r_{\min}(C(t))$ is the kill rate of the most resistant subpopulation as a function of antibiotic concentration $C(t)$, typically an expression of the type $r_{\min}(C) = K_k \frac{C^H}{C^H + C_{50}^H}$ (Wagner 1968, Jusko 1971, Giraldo, Vivas et al. 2002) where K_k is the maximal kill rate achieved as $C \to \infty$; C_{50} is a constant equal to the antimicrobial agent concentration at which 50% of the maximal kill rate is achieved; and H is the Hill exponent (Hill 1910), corresponding to how inflected r is as a function of C.

To estimate model parameters, measurements of $N_{\text{live}}(t)$ can be typically obtained by drawing small samples from the bacterial population at distinct points in time and using standard plating methods (Sanders 2012). As already mentioned, this measurement approach is well established but is laborious, time-consuming, and can reasonably produce measurements at only a few distinct points in time. By contrast, simple optical methods produce an essentially continuous signal for the bacterial population size over time. The Achilles heel of these methods is that while they produce a signal for a bacterial population in growth that is easy to interpret by inspection. when the bacterial population of live cells is in decline (because of antibiotic exposure) the OD signal produced is practically impossible to interpret by inspection as it appears to contain little or no information (Fig. 1).

Therefore, there is an incentive to develop equations that capture the pharmacodynamics of the combined population of both live and dead cells exposed to an antibiotic, as counterparts of Eqs. (1) and (2). The utility of such equations would be in inferring profiles over time for *live* cell counts from measurements of *total* (both live and dead) cell counts in a population. That information would guide decisions about effective use of antibiotics, particularly to eradicate bacterial populations that exhibit varying degrees of resistance to one or multiple antibiotics. The development of such equations is discussed in the next section.

2.2. Antibiotic agent

Levofloxacin (LVX) powder was a gift from Achaogen (South San Francisco, CA). A stock solution at 1024 μg/mL in sterile water has been prepared ahead of time and stored in −70°C. For each experimental study, the drug was diluted to the optimum concentration through standard lab techniques.

2.3. Microorganism

A laboratory reference wild type *Acinetobacter baumannii* (AB), ATCC BAA747, was utilized in the study. The bacteria were stored at −70°C in Protect® vials. Before the experiment, the bacteria were subcultured at least twice on 5% blood agar plates for 24 hours at 35°C and fresh colonies were used. The susceptibility (MIC) to LVX was previously found to be 0.25 μg/mL.

2.4. OD measurements

Real time measurements of the bacterial population size are provided by an optical instrument (model 216Dx), provided by BacterioScan® (St. Louis, MO). The instrument is currently functional with additional development for various improvements underway. The instrument uses laser light scattering coupled with traditional OD measurements to provide a quantitative measure of particle (e.g. bacterial) density in liquid samples. Prepared samples were loaded into custom, sterilized cartridges and inserted into instruments for automated optical profiling. The instrument utilizes a 650 nm wavelength laser that is passed through the liquid sample (with a 2.5 cm pathlength) and collects both the scattered light as well as the unscattered light (no particle interaction) signals. Using a proprietary algorithm, these signals are converted to numeric values and scaled to bacterial colony forming units per milliliter (CFU/ml) based on average size and density standards for typical bacterial cells. In its current version, the instrument allows for simultaneous measurements of 16 individual combinations of antibiotic and bacterial population in suspension maintained at 35°C. Full computer connectivity allows continuous monitoring, storage, and transfer of all measurements.

2.5. Bacterial susceptibility studies

Bacteria were initially grown in a temperature regulated shaker bath to log phase growth and diluted to a concentration of $10^5 - 10^{5.5}\frac{\text{CFU}}{\text{mL}}$. The initial target concentration was estimated by absorbance values at 630 nm. Samples of the bacterial population at the desired initial concentration were transferred to six temperature regulated flasks with cation adjusted Mueller Hinton broth and LVX concentrations of {0, 0.5, 2, 8, 16, 32} × MIC. Serial samples were taken in duplicate from each flask at 0, 2,4, 8 and 24 hours. Each sample containing antibiotic was first centrifuged to remove the supernatant antibiotic solution, replace it with an equal volume of sterile saline to minimize drug carryover effect, and was subsequently plated quantitatively to determine viable bacterial burden. The preceding procedure was repeated three times on different days.

2.6. Optical instrument susceptibility studies

Bacteria were initially grown in a temperature regulated shaker bath to log phase growth and diluted to a concentration of $10^5 - 10^{5.5}\frac{\text{CFU}}{\text{mL}}$. The initial target concentration was estimated by absorbance values at 630 nm. Samples of the bacterial population at the desired initial concentration were transferred to 4 temperature regulated covets inside the optical instrument with cation adjusted Mueller Hinton broth and LVX concentrations of {0, 0.5, 2, 8} × MIC. The instrument took serial samples automatically from each flask approximately every 1 minute for 48 hours. The preceding procedure was repeated three times on different days.

2.7. Data fit

Nonlinear regression was used for parameter estimation. Parameters were estimated in two platforms: Matlab® (function “fitnlm” of the Optimization Toolbox) and MS Excel® (Generalized Reduced Gradient in the Solver Add-in). Multiple starting points were used to

avoid convergence to local optima. Eq. (1) was used to fit data from the viability plating experiments described above. Similarly Eq. (17) (developed below in Results) was used to fit data from OD instruments.

3. Results

3.1. Mathematical modeling

We proceed to the step-by-step derivation of the dynamics and analytical expression for the entire size (both live and dead cells) of a heterogeneous bacterial population exposed to an antibiotic at a time-invariant concentration. This is a typical setting in time-kill experiments, as the data it produces, particularly if successfully modeled, can be well used to analyze the effect of antibiotics at time-varying concentrations corresponding to realistic pharmacokinetics of clinical significance (Nikolaou, Schilling et al. 2007).

It can be shown (Bhagunde, Nikolaou et al. 2015) that when a heterogeneous bacterial population is exposed to an antibiotic, the dynamics of the population of live bacterial cells becomes

$$\frac{dN_{\text{live}}}{dt} = \underbrace{K_g\left[1-\frac{N_{\text{live}}(t)}{N_{\max}}\right]N_{\text{live}}(t)}_{\text{Net physiological growth}} - \underbrace{\mu(t)N_{\text{live}}(t)}_{\substack{\text{Kill rate induced}\\ \text{by antibiotic}}} \tag{4}$$

with $\mu(t)$ as in Eq. (2).

Similarly, the dynamics of the population of dead cells becomes

$$\frac{dN_{\text{dead}}}{dt} = \underbrace{K_d N_{\text{live}}(t)}_{\substack{\text{physiological}\\ \text{death}}} + \underbrace{\mu(t)N_{\text{live}}(t)}_{\substack{\text{Killing induced}\\ \text{by antibiotic}}} = (K_d+\mu(t))N_{\text{live}}(t) \tag{5}$$

Adding Eqs. (4) and (5) yields the following equation for the entire population

$$N_{\text{total}} = N_{\text{live}} + N_{\text{dead}} \tag{6}$$

of live and dead cells:

$$\begin{aligned}\frac{dN_{\text{total}}}{dt} &= \frac{d(N_{\text{live}}+N_{\text{dead}})}{dt}\\ &= \underbrace{K_g\left[1-\frac{N_{\text{live}}(t)}{N_{\max}}\right]N_{\text{live}}(t)}_{\text{Net physiological growth}} - \underbrace{\mu(t)N_{\text{live}}(t)}_{\substack{\text{Kill rate induced}\\ \text{by antibiotic}}} + \underbrace{K_d N_{\text{live}}(t)}_{\text{Death}} + \underbrace{\mu(t)N_{\text{live}}(t)}_{\substack{\text{Kill rate induced}\\ \text{by antibiotic}}}\\ &= \left(K_d + K_g\left[1-\frac{N_{\text{live}}(t)}{N_{\max}}\right]\right)N_{\text{live}}(t)\\ &= \left(K_b - K_g\frac{N_{\text{live}}(t)}{N_{\max}}\right)N_{\text{live}}(t)\end{aligned} \tag{7}$$

where the connection between the constants K_g, K_b, and K_b is discussed in APPENDIX A

Combination of Eqs. (2), (4), and (7) immediately implies

$$\frac{dN_{\text{live}}}{dt} = \left(-K_g \frac{N_{\text{live}}(t)}{N_{\max}} + K_g - r_{\min} - \lambda a e^{-at}\right) N_{\text{live}}(t) \tag{8}$$

$$\begin{aligned} \frac{dN_{\text{total}}}{dt} &= \left(K_g\left[1 - \frac{N_{\text{live}}(t)}{N_{\max}}\right] + K_d\right) N_{\text{live}}(t) \\ &= \left(-K_g \frac{N_{\text{live}}(t)}{N_{\max}} + K_b\right) N_{\text{live}}(t) \end{aligned} \tag{9}$$

Note that from the above Eq. (8) it is clear that the bacterial population can be eventually eradicated if and only if

$$r_{\min} > K_g \tag{10}$$

The above Eqs. (8) and (9) can be solved analytically to provide closed form expressions for $N_{\text{total}}(t)$, as discussed next.

3.1.1. $N_{\text{total}}(t)$ for growing bacterial population (no antibiotic)—In the absence of antibiotic, Eq. (8) yields $\frac{dN_{\text{live}}}{dt} = K_g[1 - \frac{N_{\text{live}}(t)}{N_{\max}}]N_{\text{live}}(t)$ which, in turn, yields

$$N_{\text{live}}(t) = N_0 \frac{1}{\frac{N_0}{N_{\max}} + \mathrm{e}^{-K_g t}\left(1 - \frac{N_0}{N_{\max}}\right)} \tag{11}$$

(Incidentally, Eq. (11) is the counterpart of Eq. (1) for $r_{\min} = \lambda = 0$.) Substituting the above $N_{\text{live}}(t)$ into Eq. (9) and integrating yields

$$\begin{aligned} \frac{N_{\text{total}}(t)}{N_0} &= \frac{1}{\frac{N_0}{N_{\max}} + e^{-K_g t}\left(1 - \frac{N_0}{N_{\max}}\right)} \\ &+ \frac{N_{\max}}{N_0}\frac{K_d}{K_g}\ln\left[(e^{K_g t} - 1)\frac{N_0}{N_{\max}} + 1\right] \end{aligned} \tag{12}$$

Note the asymptotic behavior of the above Eq. (12):

- For $t \approx 0$ with an initial bacterial population size well below its saturation point, we have $\frac{N_0}{N_{\max}} \approx 0$ which implies

$$\frac{N_{\text{total}}(t)}{N_0} \approx \left(\left(1 + \frac{K_d}{K_g}\right)e^{K_g t} - \frac{K_d}{K_g}\right) \tag{13}$$

Typical profiles for each of Eq. (11), (12), and (13) are shown in Fig. 2.

- For $t \to \infty$ we get

$$\frac{N_{\text{total}}(t)}{N_0} \approx \frac{N_{\max}}{N_0} K_d t \tag{14}$$

3.1.2. General bacterial population exposed to antibiotic—In the presence of an antibiotic, Eq. (8) eventually yields (APPENDIX B)

$$\frac{N_{\text{total}}(t)}{N_0} = \frac{e^{\lambda(e^{-at}-1)+(K_g-r_{\min})t}}{1+K_g\frac{N_0}{N_{\max}}\frac{e^{-\lambda}}{a}\lambda\frac{K_g-r_{\min}}{a}\int_{\lambda e^{-at}}^{\lambda} z^{-1+\frac{r_{\min}-K_g}{a}}e^z dz} + \int_0^t \frac{(K_d+r_{\min}+\lambda a e^{-a\tau})e^{\lambda(e^{-a\tau}-1)+(K_g-r_{\min})\tau}}{1+K_g\frac{N_0}{N_{\max}}\frac{e^{-\lambda}}{a}\lambda\frac{K_g-r_{\min}}{a}\int_{\lambda e^{-a\tau}}^{\lambda} z^{-1+\frac{r_{\min}-K_g}{a}}e^z dz} d\tau \tag{15}$$

Note that when the initial population is far from its saturation point, i.e. $\frac{N_0}{N_{\max}} \approx 0$, then Eq. (8) yields

$$\frac{N_{\text{live}}(t)}{N_0} = e^{\lambda(e^{-at}-1)+(K_g-r_{\min})t} \tag{16}$$

which implies that Eq. (15) can be simplified as

$$\frac{N_{\text{total}}(t)}{N_0} = e^{\lambda(e^{-at}-1)+(K_g-r_{\min})t} + e^{-\lambda}\lambda^{\frac{K_g-r_{\min}}{a}}\left(\frac{K_d+r_{\min}}{a}\int_{\lambda e^{-at}}^{\lambda} z^{-1+\frac{r_{\min}-K_g}{a}}e^z dz + \int_{\lambda e^{-at}}^{\lambda} z\frac{r_{\min}-K_g}{a}e^z dz\right) \tag{17}$$

3.2. Experimental data collection and processing

To illustrate the applicability of the mathematical modeling framework presented above, we present the following results. The central ideas behind these results are as follows:

- For each time-invariant antibiotic concentration, experimental data from *OD measurements* of $N_{\text{total}}(t)$ were used with the modeling equations developed above to fit parameters, using Eq. (17), and then use these parameter estimates to infer the live cell population count over time, $N_{\text{live}}(t)$, using Eq. (1). The outcome is shown in Fig. 3 with parameter values shown in Table 1. Note that Eqs. (2) and (3) were used to express the parameters $r_{\min}$ and λ in Eqs. (1) and (17) as

$$r_{\min} = \mu(0) - \frac{\sigma(0)^2}{a} \tag{18}$$

$$\lambda = \frac{\sigma(0)^2}{a^2} \tag{19}$$

to improve the convergence properties of numerical parameter estimation algorithms.

- For the same time-invariant antibiotic concentrations (0-8 MIC), samples from corresponding cultures were collected at selected times (1, 2, 4, 8, and 24 hours) and plated, to have *direct (viability plating) measurements* of N_{live} at these select times. The viability plating data were fit by Eq. (1) to produce direct estimates of $N_{\text{live}}(t)$ for all times t. The outcome for $N_{\text{live}}(t)$ is shown in Fig. 4 and can be directly compared to the $N_{\text{live}}(t)$ shown in Fig. 3.
- To further compare OD data and plating data, parameter estimates from fitting the plating data of $N_{\text{live}}(t)$ using Eq. (1) were used in Eq. (17) (with the addition of an average value for K_d, Table 1) to infer $N_{\text{total}}(t)$ for plating data. The outcome is shown in Fig. 5.
- Finally, to test the predictive ability of the proposed model when data are available over shorter periods of time, we used Eq. (17) to estimate N_{live} by selecting part of the data produced by OD for N_{total} over increasingly shorter periods of time, namely 24, 12, 9, and 6 hours. The outcome, which is counterpart of Fig. 3 for data of the shorter time spans indicated above, is shown in Fig. 6 through Fig. 9, with corresponding parameter estimates shown in Table 1.

4. Discussion

The main focus of the work presented was to address a basic question, which, in the context discussed, can be summarized as follows:

> "Given that bacterial cell counts assessed over time by OD measurements *never decline*, as the counts include *both live and dead* cells, is it feasible to glean the trend of *live* cell counts from OD measurements alone over time? In particular, can regrowth of live cells following initial decline be gleaned from OD data alone?"

Comparison of the results in Fig. 3 through Fig. 5 indicates that this is feasible (Figs. 7 and 8). Specifically, it can be observed that the regrowth of the resistant bacterial subpopulation, robustly identified by plating experiments at all antibiotic concentrations (0.5, 2, 8 × MIC) is also identified from OD data alone by application of the proposed mathematical modeling method of section 2 in almost all cases, except only for OD data collected over 24h at 8 × MIC and, quite expectedly, for OD data collected over 6h at (2, 8) × MIC. In fact, analysis of that last set was performed with the intent to explore how short a time interval can be successfully handled by the proposed method for inferring $N_{\text{live}}(t)$ from $N_{\text{total}}(t)$.

Note that R^2 values are reported with the intent to offer a quantitative sense of completeness, but they should be interpreted with caution when fitting OD measurements, because these measurements contain systematic errors. For example, in the few cases where R^2 becomes very low, the culprit is a slightly declining part of relatively flat line, an artifact of the instrument used, which our mathematical model cannot fit well, as it has been built to only represent increasing or flat lines, for the fundamental reasons already explained.

Also note that because estimates of K_d could not be obtained directly from plating data, they were obtained from fitting Eq. (17) to data produced by the OD instrument, with all remaining parameters set at their values estimated from plating data.

It is worth deciphering in a narrative how the equations of the proposed mathematical method manage to identify a declining bacterial population when there is never any such indication in the original data by inspection. The key is that the bacterial population is not homogeneous, and subpopulations respond differently to antibiotic exposure: At a given antibiotic concentration, resistant subpopulations continue growth, perhaps at reduced rate, while susceptible subpopulations decline. The net effect is net growth of both live and dead bacterial cell counts combined, but at a rate lower than natural growth, as dead cells do not disappear but do not grow either. This trend offers useful information early on, long before a bacterial population reaches its saturation point. This partly offsets the experimental shortcomings of the instrument used, which introduces small systematic errors over time. Thus, combining everything, the equations developed in section 2 (most notably Eq. (17)) allow for fit of the data by a corresponding model and subsequent inference of $N_{\text{live}}(t)$, which is the outcome produced by the method.

The fundamental capability described above creates the potential for OD measurements to be routinely used as a highly efficient tool for automatically discerning the pharmacodynamics of bacteria/antibiotic interaction in a short period of time and for using the outcome towards the rapid design of personalized therapeutic treatments.

The robustness of the results presented here is better appreciated in view of the fact that small systematic errors are evident in all OD measurements collected, as the associated OD measurement technology is under development. For example, the OD measurement growth curves in Fig. 6 through Fig. 9 exhibit a temporary reduction in growth rate starting at around 4 hours. The growth rate resumes its previous value at around 6 hours. Finally, it starts to plateau at around 10 hours. The growth rate fluctuation from an initial value to a lower one and back is purely an artifact of the instrument used, as different optical methods (diffraction and absorption) are used for cell counting in different time regimes. Artificial fluctuations are also noticed in the time-kill curves at around 6 hours and 24–35 hours for 1/2 × MIC, at 12 hours for the 2 × MIC curve and slightly later for the 8 × MIC curve. The sources of these systematic errors vary. One is that dead cells decompose over time, thus changing the optical signature of the cell suspension. Another is the non-uniformity of concentration of cells in suspension used in the instrument. Yet another one is that antibiotics can induce morphological changes to the bacteria; for instance, fluoroquinolones, as levofloxacin, may induce filaments when exposed to concentrations close to the MIC, which increases the size but not the number of bacteria, thus inadvertently changing again

the optical signature observed.[1] As expected, model fits to data collected over different time periods are impacted by these fluctuations. Nevertheless, the results show remarkable robustness, and one can only expect improvements with the availability of better OD instruments.

Finally, it should also be emphasized that the information contained in the fitted model could be used in the design of effective therapies against challenging infections, e.g. by ensuring that $r_{\min} > K_g$ or by ensuring that $\frac{1}{T}\int_0^T r_{\min}(C(t))dt > K_g$ is satisfied. This underscores the important role of using the proposed mathematical modeling framework to extract information on a declining population from measurements that could not possibly provide a direct detection of such decline, and to use such information effectively for therapeutic purposes.

5. Conclusion

A mathematical model-based method was developed to glean in vitro pharmacodynamics from otherwise unusable OD measurements collected in time-kill experiments of bacterial populations exposed to antibiotics. The model-based method was applied to experimental OD measurements over time, and produced estimates of live bacteria count patterns in agreement with count patterns produced manually by a standard plating method at a few sampling points. The mathematical model-based method developed here helps retain all of the advantages associated with OD measurements, while removing their basic disadvantage, namely their inability to distinguish between live and dead cells and thus to track the size of a bacterial population in decline from exposure to antibiotics. This model-based method paves the way towards rapid systematic design of effective personalized dosing regimens against resistant bacteria. As development of OD measurement technology progresses further, e.g. by simplifying calibration or by extending the dynamic range (López, Prieto et al. 2004, Mytilinaios 2012, Pla, Oltra et al. 2015), it is anticipated that use of the model-based method presented here will prove useful at improving therapeutic outcomes in treatment of resistant clinical infections.

Acknowledgements

The Institute of Allergy and Infectious Diseases of the National Institutes of Health under award number R01AI140287 supported the research reported in this publication.

100% of the project costs were financed with Federal money.

The content is solely the responsibility of the authors and does not necessarily represent the official views of the National Institutes of Health.

Funding sources had no involvement in study design; in the collection, analysis and interpretation of data, nor in the writing of the report nor in the decision to submit the article for publication.

[1] We gratefully acknowledge an anonymous reviewer for bringing this to our attention.

Appendix A.: Connection between K_g, K_b, and K_d

In the absence of an antibiotic, the growth dynamics of a bacterial population is characterized by

$$\begin{aligned}\frac{dN_{\text{live}}}{dt} &= \underbrace{K_b\left[1-\frac{N_{\text{live}}(t)}{N_c}\right]N_{\text{live}}(t)}_{\text{Physiological birth}} - \underbrace{K_d N_{\text{live}}(t)}_{\text{Physiological death}} \\ &= \underbrace{(K_b-K_d)}_{K_g}\left[1-\frac{K_b}{K_b-K_d}\frac{N_{\text{live}}(t)}{N_c}\right]N_{\text{live}}(t) \\ &= \underbrace{K_g\left[1-\frac{N_{\text{live}}(t)}{N_{\max}}\right]N_{\text{live}}(t)}_{\text{Net physiological growth}}\end{aligned} \tag{A.1}$$

where

$$N_{\max} = N_c\frac{K_b-K_d}{K_b} = N_c\frac{K_g}{K_b} \tag{A.2}$$

and

$$K_g = K_b - K_d \tag{A.3}$$

Appendix B.: Derivation of Eq. (15)

Eq. (8) can be solved analytically to yield

$$\begin{aligned}\frac{N_{\text{live}}(t)}{N_0} &= \frac{e^{\lambda(e^{-at}-1)+(K_g-r_{\min})t}}{1+K_g\frac{N_0}{N_{\max}}\int_0^t e^{\lambda(e^{-a\tau}-1)+(K_g-r_{\min})\tau}d\tau} \\ &= \frac{e^{\lambda(e^{-at}-1)+(K_g-r_{\min})t}}{1+K_g\frac{N_0}{N_{\max}}\frac{e^{-\lambda}}{a}\lambda\frac{K_g-r_{\min}}{a}\int_{\lambda e^{-at}}^{\lambda} z^{-1+\frac{r_{\min}-K_g}{a}}e^z dz}\end{aligned} \tag{B.1}$$

with $\lambda > 0$, $a > 0$, $r_{\min} > 0$. Therefore

$$\begin{aligned}&\frac{dN_{\text{total}}}{dt} = \frac{dN_{\text{live}}}{dt} + \frac{dN_{\text{dead}}}{dt} \Rightarrow \\ &\frac{N_{\text{total}}(t)}{N_0} = \frac{N_{\text{live}}(t)}{N_0} + \int_0^t \frac{dN_{\text{dead}}/N_0}{d\tau}d\tau = \frac{N_{\text{live}}(t)}{N_0} \\ &+ \int_0^t (K_d+\mu(\tau))\frac{N_{\text{live}}(\tau)}{N_0}d\tau\end{aligned}$$

which implies Eq. (15).

Appendix C.: Parameter estimation from experimental plating data

See Table C.1.

Table C.1

Parameter estimation for each plating experiment and derivation of average parameters for each concentration of antimicrobial agent.

Source: Parameter	Plating experiment 1 Values	Plating experiment 2 Values	Plating experiment 3 Values	Average values
Time Growth Placebo				
log N_{max}	8.8 ± 0.1	8.2 ± 0.01	8.4 ± 0.05	8.5 ± 0.06
K_g	1.8 ± 0.2	2.2 ± 0.03	2.3 ± 0.012	2.1 ± 0.13
LogNo	5.1 ± 0.2	5.3 ± 0.02	5.0 ± 0.08	5.2 ± 0.09
K_d	4.0**	4.0**	4.0**	4**
Time Kill 1/2 MIC				
$\mu(0)$	8.1 ± 0.3	12 ± 0.3	4.0 ± 0.7	8.0 ± 0.3
$\sigma(0)$	3.1 ± 0.1	4.5 ± 0.1	0.74 ± 0.36	3.0 ± 0.1
α	1.4 ± 0.1	2.1 ± 0.1	0.24 ± 0.9	1.3 ± 0.1
Time Kill 2 MIC				
$\mu(0)$	15 ± 0.6	11 ± 0.4	13 ± 0.53	13 ± 0.5
$\sigma(0)$	4.6 ± 0.1	3.6 ± 0.1	4.0 ± 0.12	4.0 ± 0.1
α	1.6 ± 0.1	1.5 ± 0.1	1.5 ± 0.12	1.5 ± 0.1
Time Kill 8 MIC				
$\mu(0)$	17 ± 1.1			17 ± 1.1
$\sigma(0)$	4.3 ± 0.2			4.3 ± 0.2
α	1.2 ± 0.2			1.2 ± 0.2

References

Alakomi HL, Mättö J, Virkajärvi I, Saarela M, 2005. Application of a microplate scale fluorochrome staining assay for the assessment of viability of probiotic preparations. J. Microbiol. Methods 62 (1), 25–35. [PubMed: 15823392]

Andrews JM, 2001. Determination of minimum inhibitory concentrations. J. Antimicrob. Chemother 48, 5–16. [PubMed: 11420333]

Bhagunde PR, Nikolaou M, Tam VH, 2015. Modeling heterogeneous bacterial populations exposed to antibiotics: The logistic-dynamics case. AIChE J. 61 (8), 2385–2393.

Blair JMA, Webber MA, Baylay AJ, Ogbolu DO, Piddock LJV, 2015. Molecular mechanisms of antibiotic resistance. Nat. Rev. Microbiol 13 (1), 42–51. [PubMed: 25435309]

Blanquart F, Lehtinen S, Lipsitch M, Fraser C, 2018. The evolution of antibiotic resistance in a structured host population. J. R. Soc. interface 15 (143).

Blaser MJ, 2016. Antibiotic use and its consequences for the normal microbiome. Science 352 (6285), 544–545. [PubMed: 27126037]

Crofts TS, Gasparrini AJ, Dantas G, 2017. Next-generation approaches to understand and combat the antibiotic resistome. Nat. Rev. Microbiol 15 (7), 422–434. [PubMed: 28392565]

Czaplewski L, Bax R, Clokie M, Dawson M, Fairhead H, Fischetti VA, Foster S, Gilmore BF, Hancock REW, Harper D, Henderson IR, Hilpert K, Jones BV, Kadioglu A, Knowles D, Olafsdottir S, Payne D, Projan S, Shaunak S, Silverman J, Thomas CM, Trust TJ, Warn P, Rex JH, 2016. Alternatives to antibiotics-a pipeline portfolio review. Lancet Infect. Dis 16 (2), 239–251. [PubMed: 26795692]

Davies J, 1994. Inactivation of antibiotics and the dissemination of resistace genes. Science 264 (5157), 375–382. [PubMed: 8153624]

Feng J, Wang T, Zhang S, Shi W, Zhang Y, 2014. An Optimized SYBR Green I/PI Assay for Rapid Viability Assessment and Antibiotic Susceptibility Testing for Borrelia burgdorferi. PLoS One 9 (11), e111809. [PubMed: 25365247]

Fischbach MA, Walsh CT, 2009. Antibiotics for Emerging Pathogens. Science 325 (5944), 1089–1093. [PubMed: 19713519]

Giraldo J, Vivas NM, Vila E, Badia A, 2002. Assessing the (a)symmetry of concentration-effect curves: empirical versus mechanistic models. Pharmacol. Ther 95, 21–45. [PubMed: 12163126]

Gracias KS, McKillip JL, 2004. A review of conventional detection and enumeration methods for pathogenic bacteria in food. Can. J. Microbiol 50 (11), 883–890. [PubMed: 15644905]

Guo R, McGoverin C, Swift S, Vanholsbeeck F, 2017. A rapid and low-cost estimation of bacteria counts in solution using fluorescence spectroscopy. Anal. Bioanal. Chem 409 (16), 3959–3967. [PubMed: 28389919]

Hasan MM, Alam MW, Wahid KA, Miah S, Lukong KE, 2016. A Low-Cost Digital Microscope with Real-Time Fluorescent Imaging Capability. PLoS One 11 (12), e0167863. [PubMed: 27977709]

Hill AV, 1910. The possible effects of the aggregation of the molecules of haemoglobin on its dissociation curves. J. Physiol 40, iv–vii.

Huh AJ, Kwon YJ, 2011. “Nanoantibiotics”: A new paradigm for treating infectious diseases using nanomaterials in the antibiotics resistant era. J. Control. Release 156 (2), 128–145. [PubMed: 21763369]

Imade GE, Badung B, Pam S, Agbaji O, Egah D, Sagay AS, Sankalé J-L, Kapiga S, Idoko J, Kanki P, 2005. Comparison of a New, Affordable Flow Cytometric Method and the Manual Magnetic Bead Technique for CD4 T-Lymphocyte Counting in a Northern Nigerian Setting. Clin. Diagn. Lab. Immunol 12 (1), 224–227. [PubMed: 15643012]

Jusko W, 1971. Pharmacodynamics of chemotherapeutic effects: dose-time-response relationships for phase-nonspecific agents. J. Pharm. Sci 60, 892–895. [PubMed: 5166939]

Kralik P, Ricchi M, 2017. A Basic Guide to Real Time PCR in Microbial Diagnostics: Definitions, Parameters, and Everything. Front. Microbiol 8 (108).

Levy SB, Marshall B, 2004. Antibacterial resistance worldwide: causes, challenges and responses. Nat. Med 10 (12), S122–S129. [PubMed: 15577930]

Lewis K, 2013. Platforms for antibiotic discovery. Nat. Rev. Drug Discov 12 (5), 371–387. [PubMed: 23629505]

Lipsitch M, Levin BR, 1997. The Population Dynamics of Antimicrobial Chemotherapy. Antimicrob. Agents Chemother 41 (2), 363–373. [PubMed: 9021193]

López S, Prieto M, Dijkstra J, Dhanoa MS, France J, 2004. Statistical evaluation of mathematical models for microbial growth. Int. J. Food Microbiol 96 (3), 289–300. [PubMed: 15454319]

McMeekin TA, Olley JN, Ross T, Ratkowsky DA, 1993. Predictive Microbiology: Theory and Application. Wiley, New York.

Morens DM, Folkers GK, Fauci AS, 2004. The challenge of emerging and re-emerging infectious diseases. Nature 430 (08 July), 242–249. [PubMed: 15241422]

Mouton JW, Dudley MN, Cars O, Derendorf H, Drusano GL, 2005. Standardization of pharmacokinetic/pharmacodynamic (PK/PD) terminology for anti-infective drugs: an update. J. Antimicrob. Chemother 55 (5), 601–607. [PubMed: 15772142]

Mytilinaios IS, Magdi Schofield, Hannah K, Lambert, Ronald JW, 2012. Growth curve prediction from optical density data. Int. J. Food Microbiol 154 (3), 169–176. [PubMed: 22280888]

Neu HC, 1992. The Crisis in Antibiotic Resistance. Science 257 (5073), 1064. [PubMed: 1509257]

Nikolaou M, Schilling AN, Vo G, Chang KT, Tam VH, 2007. Modeling of microbial population responses to time-periodic concentrations of antimicrobial agents. Ann. Biomed. Eng 35 (8), 1458–1470. [PubMed: 17431788]

Nikolaou M, Tam VH, 2006. A new modeling approach to the effect of antimicrobial agents on heterogeneous microbial populations. J. Math. Biol 52 (2), 154–182. [PubMed: 16195922]

O'Connell KMG, Hodgkinson JT, Sore HF, Welch M, Salmond GPC, Spring DR, 2013. Combating Multidrug-Resistant Bacteria: Current Strategies for the Discovery of Novel Antibacterials. Angew. Chem. Int. Ed 52 (41), 10706–10733.

Ou F, McGoverin C, Swift S, Vanholsbeeck F, 2017. Absolute bacterial cell enumeration using flow cytometry. J. Appl. Microbiol 123 (2), 464–477. [PubMed: 28600831]

Pascaud A, Amellal S, Soulas M-L, Soulas G, 2009. A fluorescence-based assay for measuring the viable cell concentration of mixed microbial communities in soil. J. Microbiol. Methods 76 (1), 81–87. [PubMed: 18926862]

Pla ML, Oltra S, Esteban MD, Andreu S, Palop A, 2015. Comparison of Primary Models to Predict Microbial Growth by the Plate Count and Absorbance Methods. Biomed Res. Int 2015, 14.

Ricchi M, Bertasio C, Boniotti MB, Vicari N, Russo S, Tilola M, Bellotti MA, Bertasi B, 2017. Comparison among the Quantification of Bacterial Pathogens by qPCR, dPCR, and Cultural Methods. Front. Microbiol 8 (1174).

Sanders ER, 2012. Aseptic Laboratory Techniques: Plating Methods. J. Vis. Exp (63) e3064. [PubMed: 22617405]

Tam V, Nikolaou M, 2011a. A Novel Approach to Pharmacodynamic Assessment of Antimicrobial Agents: New Insights to Dosing Regimen Design. PLoS Comput. Biol 7 (1), e1001043. [PubMed: 21253559]

Tam VH, Nikolaou M, 2011b. A novel approach to pharmacodynamic assessment of antimicrobial agents: new insights to dosing regimen design. PLoS Comput. Biol 7 (1), e1001043. [PubMed: 21253559]

Wagner J, 1968. Kinetics of Pharmacologic Response I. Proposed Relationships between Response and Drug Concentration in the Intact Animal and Man. J. Theoret. Biol 20, 173–201. [PubMed: 5727238]

Wang Y, Hammes F, De Roy K, Verstraete W, Boon N, 2010. Past, present and future applications of flow cytometry in aquatic microbiology. Trends Biotechnol. 28 (8), 416–424. [PubMed: 20541271]

Wang YC, Lipsitch M, 2006. Upgrading antibiotic use within a class: Trade-off between resistance and treatment success. Proc. Natl Acad. Sci 103 (25), 9655–9660. [PubMed: 16772381]

Wiegand I, Hilpert K, Hancock REW, 2008. Agar and broth dilution methods to determine the minimal inhibitory concentration (MIC) of antimicrobial substances. Nat. Protoc 3 (2), 163–175. [PubMed: 18274517]

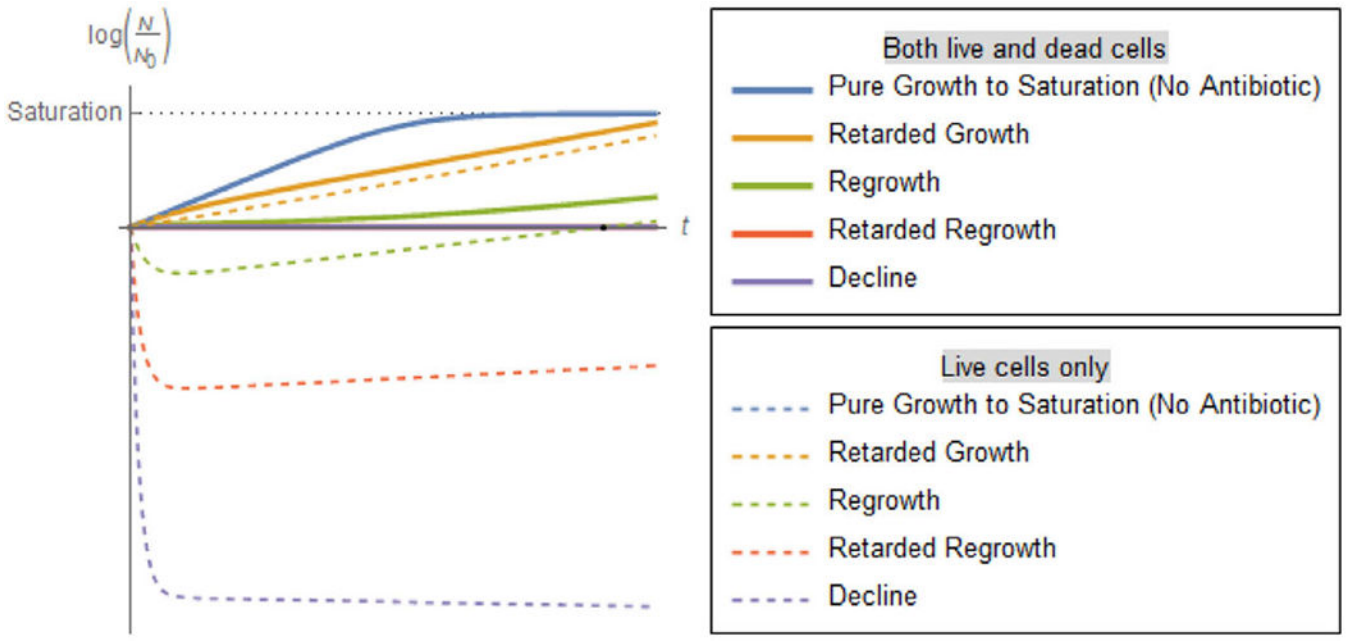

Fig. 1.

Qualitative patterns in measurements of total number of (live and dead) bacterial cells (thick lines) corresponding to populations of live bacterial cells (thin dashed lines) over time, in response to time-invariant antibiotic concentrations. A heterogeneous bacterial population is considered, comprising subpopulations of varying degrees of antibiotic resistance. As the antibiotic concentration is set at increasingly higher values, the bacterial response over time changes from full growth to the point of saturation (in the absence of antibiotic), to retarded growth, to regrowth (resulting from rapid decline of bacterial subpopulations highly susceptible to the antibiotic combined with growth of subpopulations less susceptible to the antibiotic), then retarded regrowth, and finally complete eradication of the entire bacterial population. Complete eradication will not occur if a resistant subpopulation is part of the bacterial population.

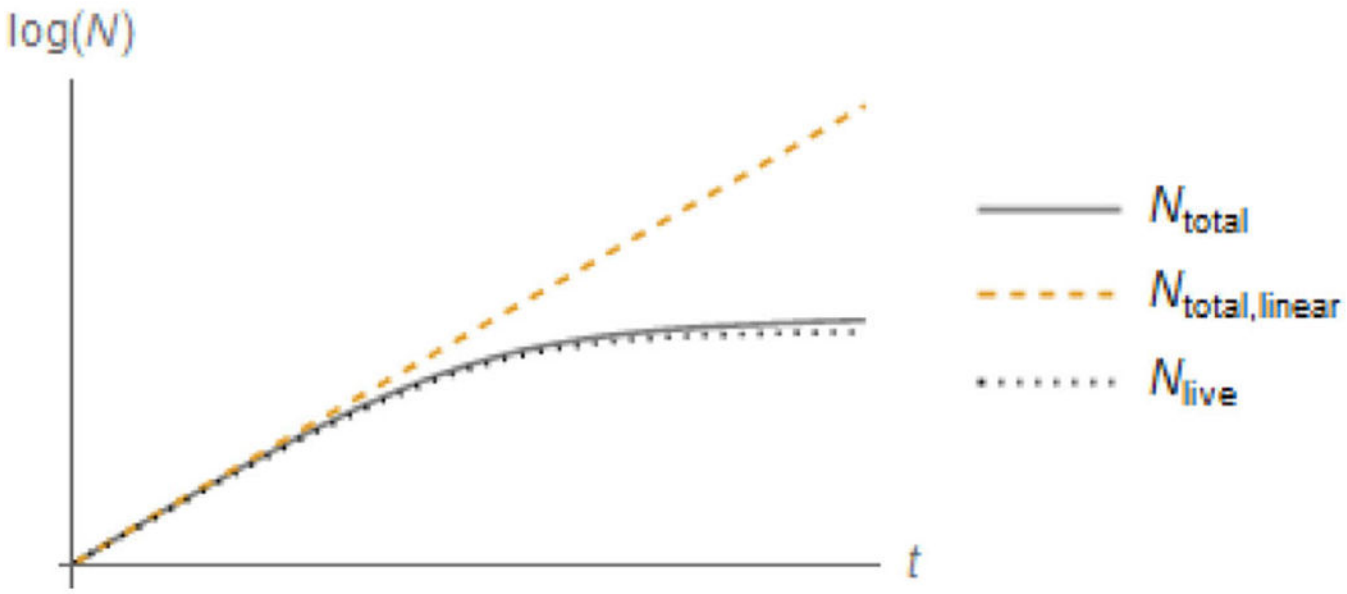

Fig. 2.
Typical profiles for each of Eqs. (11), (12), and (13).

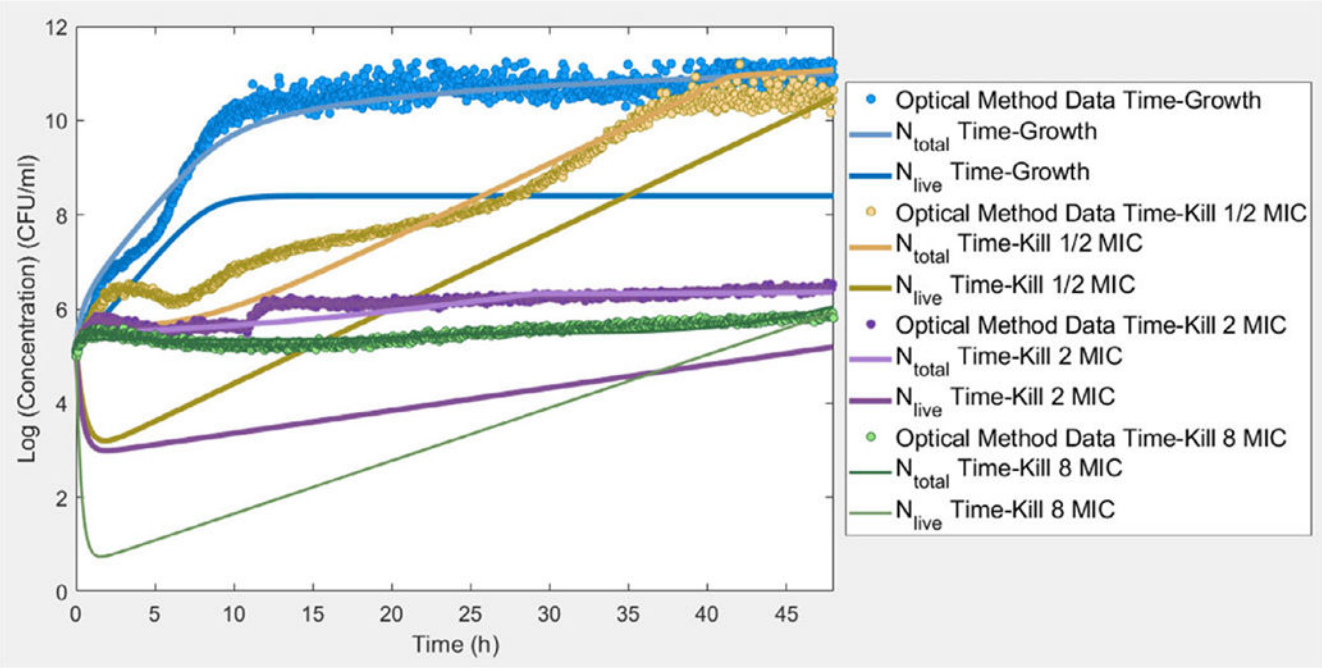

Fig. 3.

Fit of Eq. (17) to experimental data on N_{total} generated by the OD instrument for a bacterial population of AB exposed to LVX at a number of time-invariant concentrations for 48 hours, and inference of the live cell population, N_{live}, using Eq. (1).

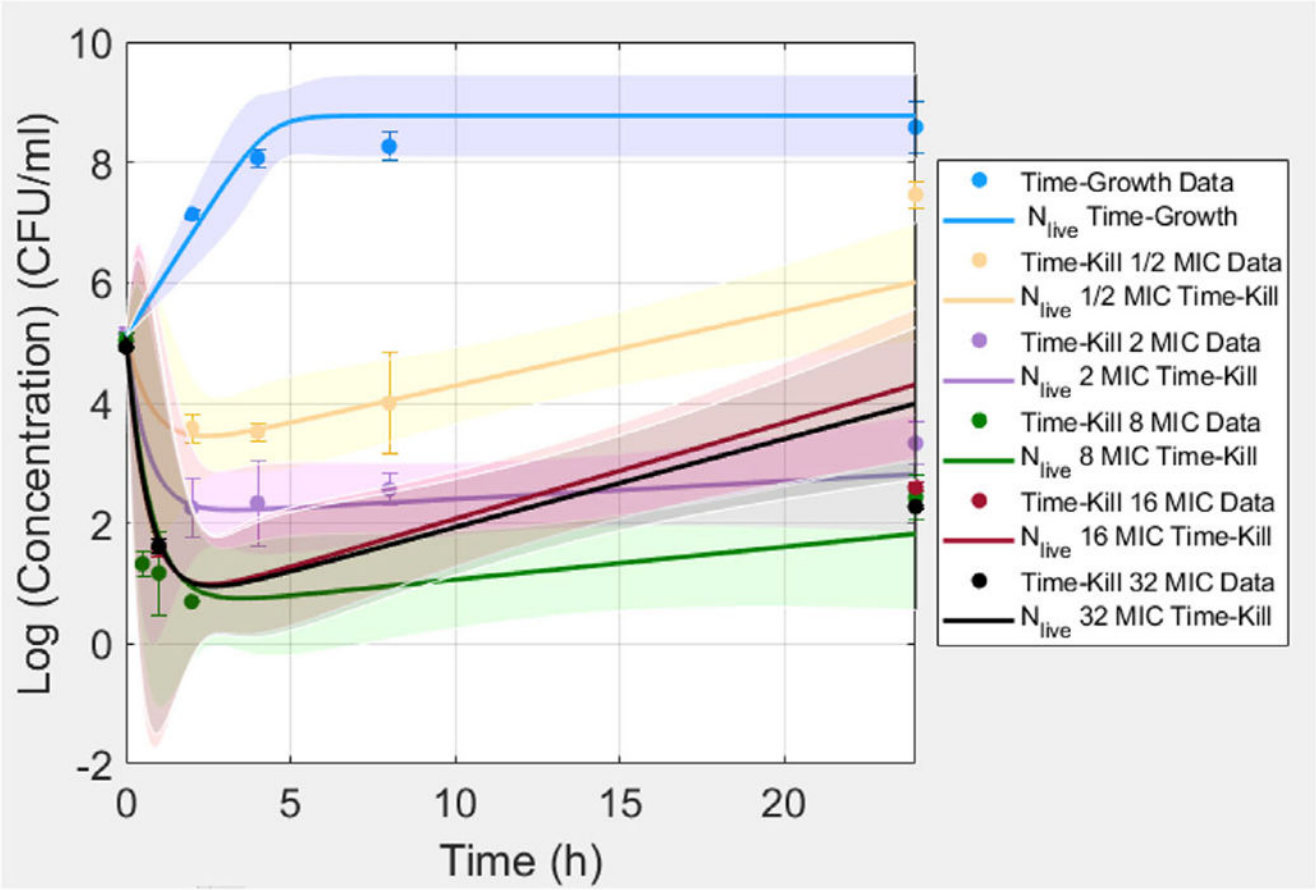

Fig. 4.

Fit of Eq. (1) to experimental data on N_{live} generated by plating for a bacterial population of AB exposed to LVX at a number of time-invariant concentrations. Standard error bands included. Note that plating data were collected at two additional concentrations in comparison to OD data, namely at 16 and 32 MIC.

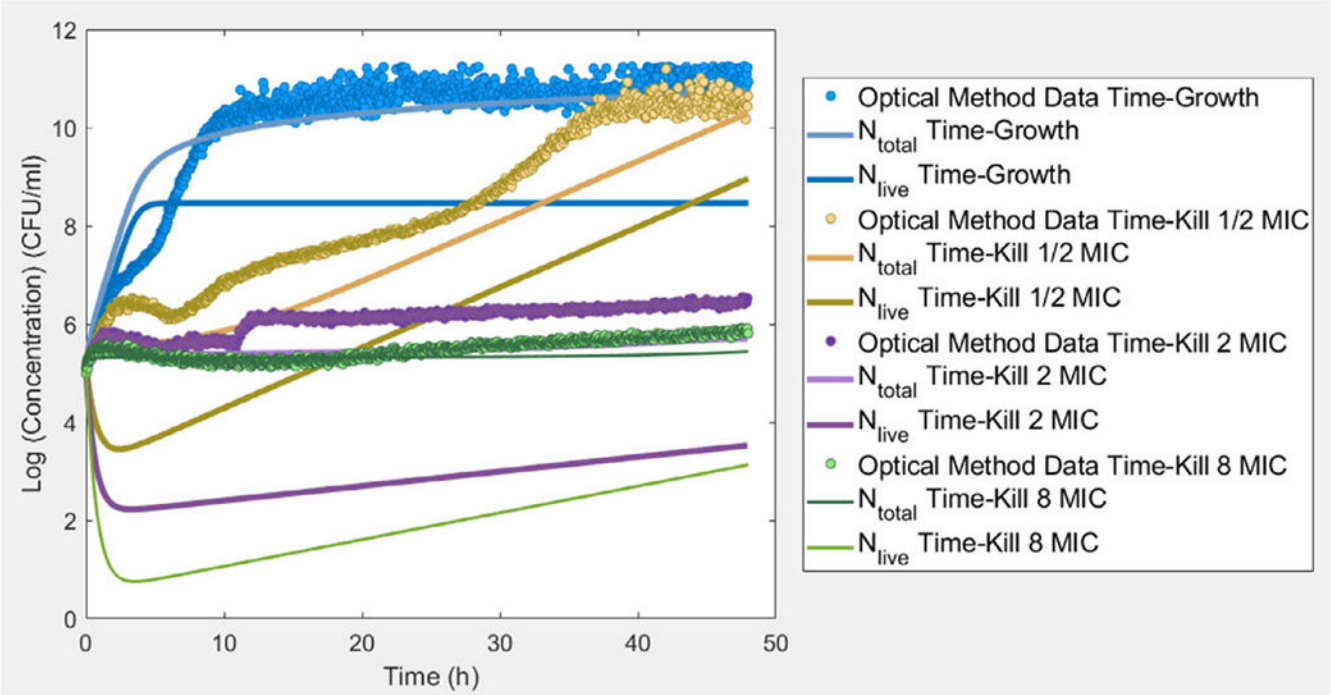

Fig. 5.

Comparison of experimental data produced by the OD instrument to the output of Eq. (1) and Eq. (17) with parameter values set by the estimates produced from the data fits reported in Table 1, referring to Fig. 4.

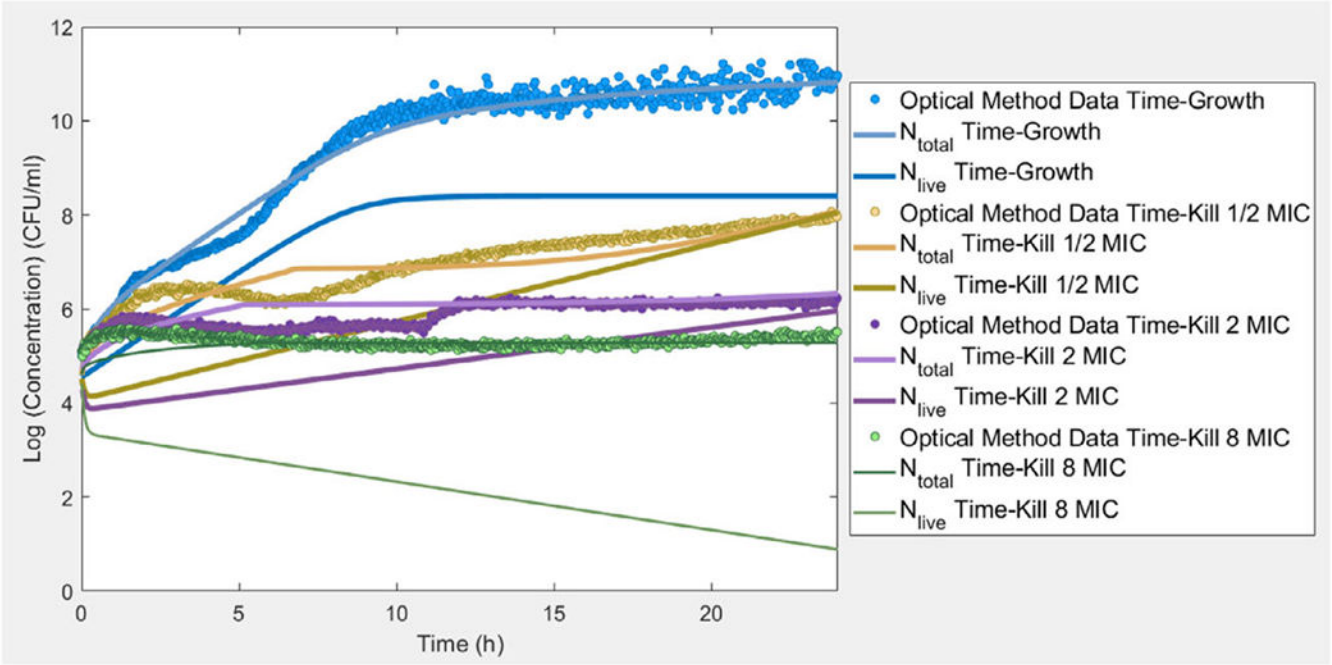

Fig. 6.

Fit of Eq. (17) to experimental data on N_{total} generated by the OD instrument for a bacterial population of AB exposed to LVX at a number of time-invariant concentrations for 24 hours, and inference of the live cell population, N_{live}, using Eq. (1).

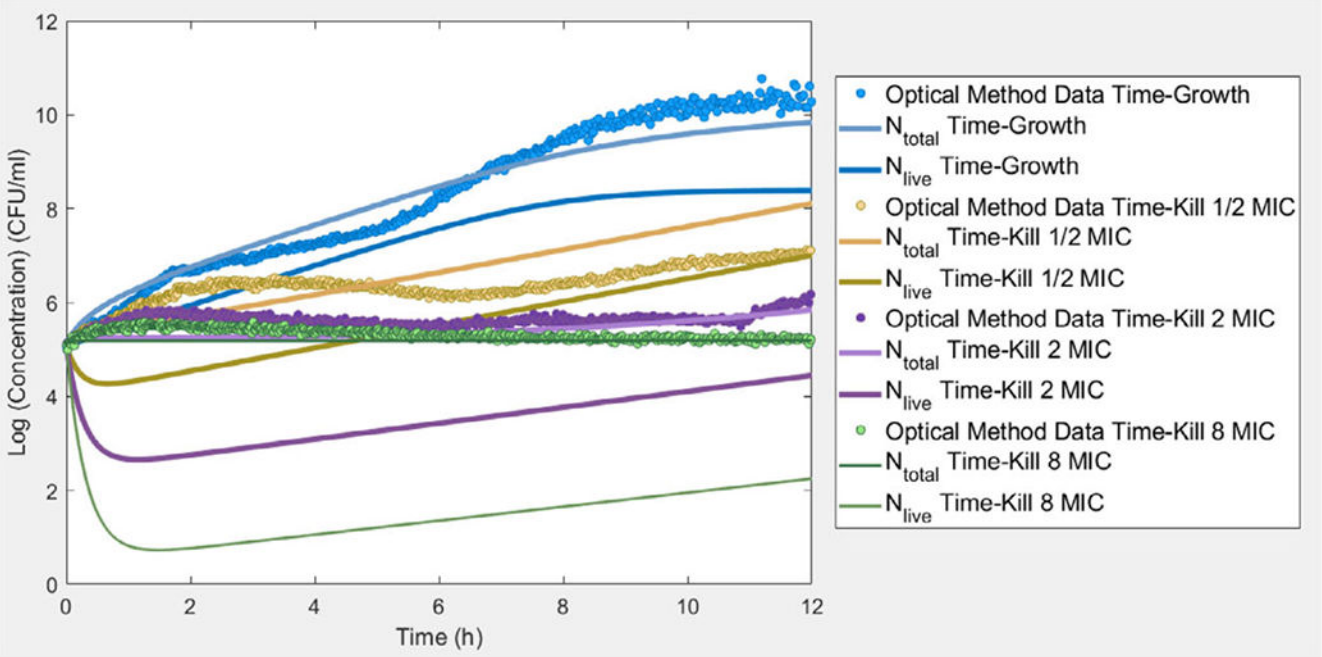

Fig. 7.

Fit of Eq. (17) to experimental data on N_{total} generated by the OD instrument for a bacterial population of AB exposed to LVX at a number of time-invariant concentrations for 12 hours, and inference of the live cell population, N_{live}, using Eq. (1).

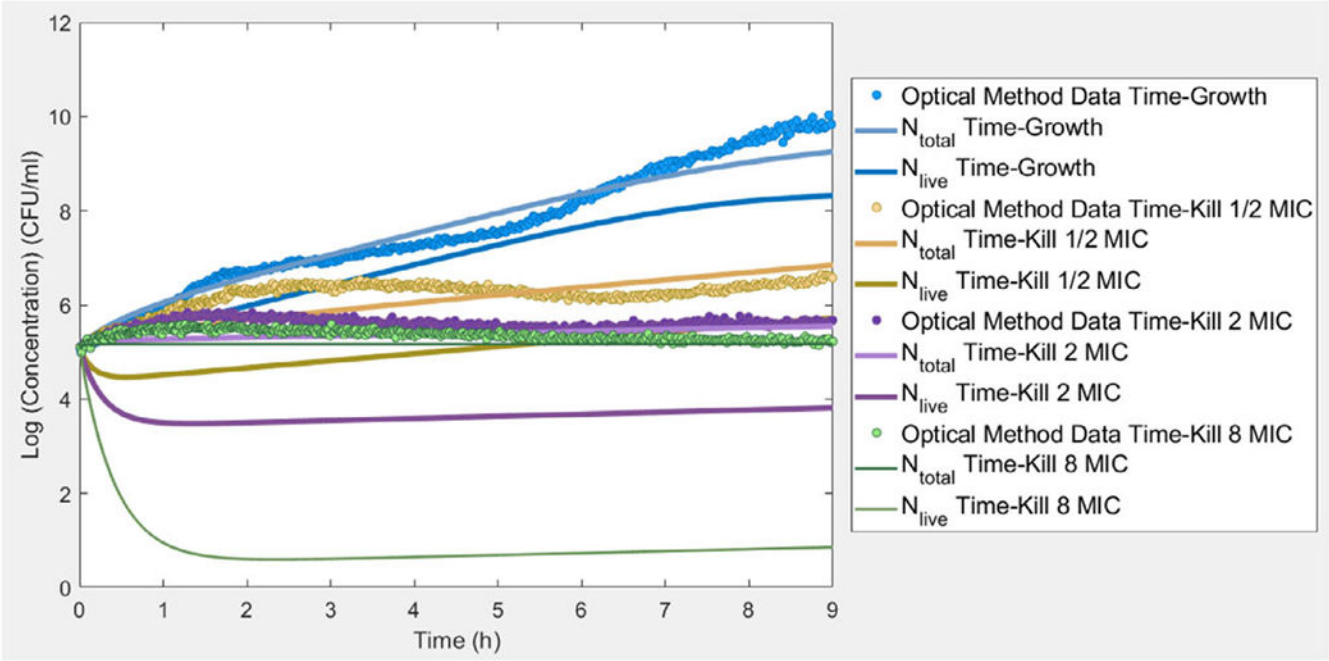

Fig. 8.

Fit of Eq. (17) to experimental data on N_{total} generated by the OD instrument for a bacterial population of AB exposed to LVX at a number of time-invariant concentrations for 9 hours, and inference of the live cell population, N_{live}, using Eq. (1).

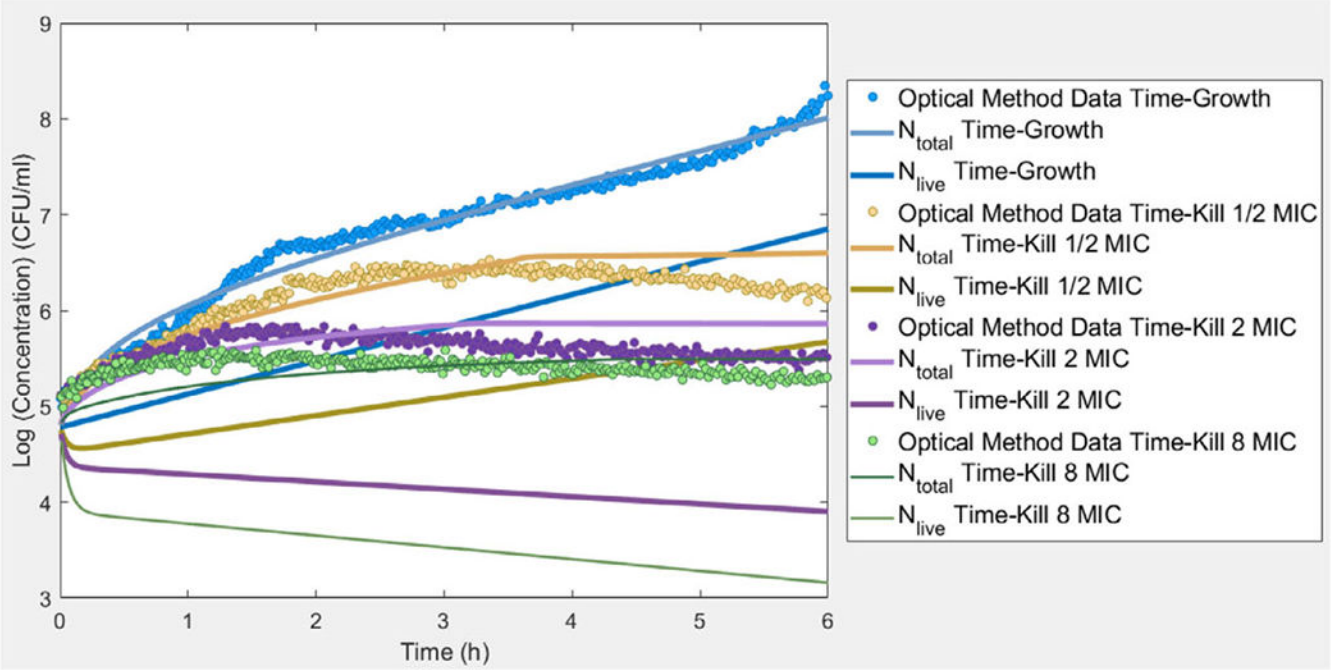

Fig. 9.

Fit of Eq. (17) to experimental data on N_{total} generated by the OD instrument for a bacterial population of AB exposed to LVX at a number of time-invariant concentrations for 6 hours, and inference of the live cell population, N_{live}, using Eq. (1).

Table 1

Parameter estimates for models in Eqs. (1) and (17).

	Instrument 48 h*	Instrument 24 h*	Instrument 12 h*	Instrument 9 h*	Instrument 6 h*	Plating**
Time Growth Placebo***						
log N_{max}	8.40 ± 0.03	8.40 ± 0.02	8.40 ± 0.06	8.40 ± 0.10	8.40 ± 4.16	8.5 ± 0.06
K_g	0.90±0.02	1.03 ± 0.01	0.98 ± 0.03	1.02±0.03	0.80 ± 0.03	2.1 ± 0.13
K_d	10.03 ± 0.75	16.88 ± 0.84	6.26 ± 0.63	3.67±0.35	10.68 ± 0.43	(4.0 +)
R^2	0.97	0.98	0.97	0.96	0.98	0.98
Time-kill 1/2 × MIC						
$\mu(0)$	9.97 ± 0.1	12.00 ± 0.02	10.94 ± 0.50	11.00 ± 0.61	12.00 ± 0.50	8.0 ± 0.3
$\sigma(0)$	4.07 ± 0.03	10.86 ± 0.01	6.81 ±0.24	7.99±0.40	15.00 ± 0.34	3.0 ± 0.1
a	1.75 ± 0.03	10.40 ± 0.02	4.41 ± 0.40	6.18 ± 0.61	19.21 ± 0.82	1.3 ± 0.1
R^2	0.97	0.82	0.66	0.48	0.86	0.94
Time-kill 2 × MIC						
$\mu(0)$	13.63 ± 0.07	23.00 ± 0.05	22.00 ± 0.24	15.00 ± 0.40	22.00 ± 5.91	13 ± 0.5
$\sigma(0)$	5.61 ± 0.02	17.42 ± 0.02	8.62 ± 0.10	7.17 ± 0.50	21.51 ± 0.83	4 ± 0.1
a	2.45±0.02	13.70 ± 0.03	3.47 ± 0.19	3.65 ± 0.19	22.01 ± 1.58	1.5 ± 0.1
R^2	0.83	0.33	0.18	0.01	0.30	0.73
Time-kill 8 × MIC						
$\mu(0)$	33.54 ± 0.001	33.54 ± 1.85	33.54 ± 0.12	26.12 ± 0.11	34 ± 4.90	17.00 ± 1.1
$\sigma(0)$	10.08 ± 0.001	19.45 ± 0.95	10.08 ± 0.03	7.73±0.03	23.06 ± 0.64	4.34 ± 0.2
a	3.09±0.001	11.72 ± 0.40	3.09 ± 0.07	2.37 ± 0.08	16.15 ± 0.49	1.2 ± 0.2
R^2	0.66	0.16	0.02	0.09	0.02	0.90

*Standard errors should be interpreted with caution, as small systematic errors are also present.

+See discussion in section 2.7 about this estimate.

**Average and standard error are shown; see APPENDIX C for further detail in regards to plating data. Parameters for plating experiments conducted at 16 and 32 MIC not reported, as corresponding experiments were not conducted with the OD instrument at these concentrations.

***Note that parameters determined at the time growth experiment are kept constant during the derivation of the time kill parameters at each antimicrobial agent concentration.